TEMPORAL VARIATION OF SCOUR AROUND CIRCULAR BRIDGE PIERS

By Umesh C. Kothyari,[1] RamChandra J. Garde,[2] and Kittur G. Ranga Raju[3]

ABSTRACT: Determination of scour depth is needed for economical design of bridge pier foundation. Currently, determination of design scour depth is mainly based on use of relationships for maximum scour depth in steady flow along with the design discharge. Computations have revealed that time taken by the design discharge to scour to its full potential is generally larger than the time for which it runs. Hence, the computation of temporal variation of scour depth should form the basis of the design. Experiments are conducted on temporal variation of scour around circular bridge piers placed in uniform, nonuniform, and stratified beds under steady and unsteady clear-water flows. Considering the primary vortex in front of the pier to be the prime agent causing scour, a procedure is developed for computing the temporal variation of scour depth under these conditions. Since the maximum scour depth is the scour depth at large time, the procedure is logically extended to obtain an expression for the same. Sediment nonuniformity and stratification are shown to have a significant effect on scour depth. The effect of these elements as well as that of unsteadiness of flow on scour depth are studied and taken into account in the proposed method of scour calculations.

INTRODUCTION

When an alluvial stream is partially obstructed by a bridge pier, the flow pattern in the channel around the pier is significantly changed. The pier produces an adverse pressure gradient just upstream from the pier. The boundary layer upstream of the pier undergoes a three-dimensional separation. The shear stress distribution around the pier is drastically changed due to the formation of a horseshoe vortex, resulting in the formation of a scour hole around the pier, which, in turn, changes the flow pattern and shear.

A majority of the scour studies have been carried out for the case of clear-water flow. Most investigators have attempted to develop relationships for the maximum scour depth in steady flow, and these are used for design. However, the flow in a river during a flood is unsteady, and discharge changes are quite rapid. Computations by Kothyari (1989) on the temporal variation of scour depth reveal that for a flood discharge of 14,000 m^3/s, sediment size of 0.17 mm, and circular pier of 2.3 m in diameter, a time of about 147 hours is required for the scour depth to develop to its equilibrium value. In natural streams at peak discharges, the unsteadiness of flow is pronounced, and one is never certain that the maximum scour depth for a given discharge would always be reached when the discharge does not run for a long time. Therefore, hydraulic design of foundations based on computations of maximum scour depth for design discharge can be erroneous. In this context, the temporal variation of scour depth assumes importance

[1]Lect., Dept. of Civ. Engrg., Univ. of Roorkee, Roorkee, India 247 667.
[2]Emeritus Fellow, Central Water and Power Res. Station, Pune, India 411 024.
[3]Prof., Dept. of Civ. Engrg., Univ. of Roorkee, Roorkee, India.

Note. Discussion open until January 1, 1993. To extend the closing date one month, a written request must be filed with the ASCE Manager of Journals. The manuscript for this paper was submitted for review and possible publication on May 4, 1990. This paper is part of the *Journal of Hydraulic Engineering*, Vol. 118, No. 8, August, 1992. ©ASCE, ISSN 0733-9429/92/0008-1091/$1.00 + $.15 per page. Paper No. 26657.

J. Hydraul. Eng., 1992, 118(8): 1091-1106

and forms an important tool for the calculation of scour depth in case of unsteady flow. Furthermore, the bed materials of rivers and canals are almost always nonuniform and/or stratified. In a rational approach for the determination of scour depth, these factors of unsteadiness, nonuniformity, and stratification need to be taken into consideration.

Several investigators have studied the temporal variation of scour depth in uniform sediments during steady flows (Nakagawa and Suzuki 1975; Hjorth 1977; Shen et al. 1965; Islam et al. 1986; Ettema 1980). Only Ettema (1980) and Tsujimoto and Motomashi (1988) have made some attempts to study the effect of sediment gradation and stratification on scour depth. Similarly, scour during unsteady flows has been studied to a limited extent by Walker (1978), Harwood (1977), and Verstappen (1978).

The main aim of the present investigation is to study the temporal variation of scour depth around circular bridge piers during steady and unsteady clear-water flows in uniform, nonuniform, and stratified sediments. Considering the paucity of data, experimental data on the temporal variation of scour depth in all these cases for clear-water flow were collected. An attempt has also been made to develop a relationship for the estimation of the maximum scour depth in clear-water flows.

Experimental Work

The experiments were conducted in a flume 30.0 m long, 1.0 m wide, and 0.60 m deep, located in the Hydraulics Laboratory of the University of Roorkee, Roorkee India. Two values of longitudinal slope, namely 6.61×10^{-4} and 1.2×10^{-3}, were used. The working section, 2.0 m long, 1.0-m wide, and 1.2-m deep where the piers were located, was 12.0 m downstream from the entrance of the flume. This reach was filled with sediment to a depth of 0.60 m below the bed level of the flume. Sediment of the same size as placed in the aforementioned recess was pasted uniformly on the remaining length of the bed of the flume. Circular pipes with diameters of 65 mm, 115 mm, and 170 mm were used as piers for the scour study, whereas concrete pipes with diameters of 80 mm and 200 mm were used for the studies on the determination of the size of the horseshoe vortex. The scour depths were measured using an electronic profile indicator MK V, manufactured in the Delft Hydraulics Laboratory, Delft, Holland. It is sensitive to bed level variations of 0.2 mm. The sediment was sand of relative density 2.65. Uniform sands having sizes 4 mm, 3 mm, 1 mm, 0.88 mm, 0.71 mm, 0.50 mm, and 0.41 mm and nonuniform sands having median size of 0.50 mm with geometric standard deviations of 1.40 and 2.0 and median size of 0.71 mm with geometric standard deviations of 2.3, 2.6, 3.2, 4.2, and 7.8 were used. Fig. 1 shows the size distribution curves of these nonuniform sediment mixtures. Two layers were used in the experiments with stratified sediments. The top layer was composed of sediment of sizes 4 mm, 3 mm, and 1 mm, whereas the bottom layer had sizes 0.41 mm and 0.71 mm. A constant thickness of 40 mm was used for the top layer.

The first series of experiments was carried out to get some idea of the size of the horseshoe vortex under different flow conditions. The horseshoe vortex is quasi-periodical and is a multiple-vortex system. Precise measurement of the size of this vortex system is difficult and was not attempted. Instead, the thickness of the separated boundary layer was measured and used as an index of the size of the primary vortex in the system. For this purpose, dye was injected into the flow at the upstream nose of the pier by

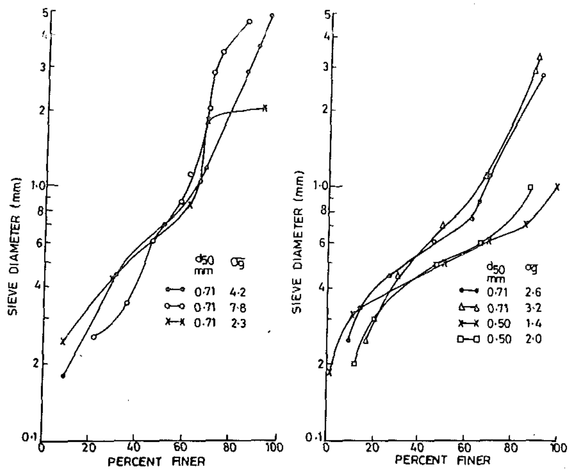

FIG. 1. Size Distribution of Nonuniform Bed Materials Used in Investigation

a 3-mm-diameter tube. The dye is deflected sideways if it is injected at or near the surface in the flow. At some depth (say, D_1) below the surface of the flow, the dye goes downward to the bed, strikes it, and is deflected sideways along the bed. Hence, the thickness of the separated boundary layer may be taken to be $D_v = D - D_1$ (where D is the flow depth). The mean diameter of the primary vortex is assumed to be D_v in further analysis. The subsequent analysis does involve introduction of empirical constants (determined by matching of the results of the proposed model with the experimental results on scour) and, hence, the fact that D_v may not precisely be the mean diameter of the vortex is unlikely to be a serious limitation of the analysis.

Before the start of each run on the temporal variation of scour depth in case of clear-water flow, the working section was made level and the pier inserted in it centrally and vertically. The area around the pier was leveled, then covered with 3-mm-thick perspex sheet. When the desired flow conditions were established using the tail gate and the inlet value, the perspex sheet was removed carefully so that no scouring occurred around the pier due to this operation. (The flow conditions for desired upstream shear stresses had been determined by a separate series of experiments conducted without the pier and the perspex sheet and with nonmovable sediment in the recess.) In all experiments with clear-water scour, the value of u_*/u_{*c} was kept between 0.82 and 0.98, i.e., less than unity. Here u_* is the shear velocity in the approach flow, and u_{*c} is the shear velocity corresponding to the threshold of sediment motion, which was determined using Shield's criterion for the median size of the sediment (Garde and Ranga Raju 1985).

The runs for steady flows were continued for a sufficiently long time, namely, up to 96 hours. Unsteady uniform flow in the flume was obtained by regulating the inlet valve and the tail gate simultaneously but in steps. During each unsteady flow run, three such steps were used.

All the data collected during the study are listed elsewhere (Kothyari 1989). In addition to the present data, those of other investigators on the temporal variation and the maximum scour depth have been used. The range of data used is given in Table 1.

TABLE 1. Range of Data

Serial number (1)	Variable (2)	Range From (3)	Range To (4)
1	diameter of primary vortex, D_v (m)	0.009	0.075
2	flow depth upstream of pier, D (m)	0.042	0.60
3	flow velocity upstream of pier, u (m/s)	0.10	1.35
4	mean size of sediment (mm)	0.24	7.8
5	pier diameter, b (m)	0.025	0.915
6	opening ratio, $\alpha = (B - b)/B$	0.5	0.98

Mathematical Model

Basic Assumptions

The following simplifying assumptions have been made regarding the mean description of geometric and hydraulic characteristics of the primary vortex.

1. Before scour begins at the pier, the primary vortex at the pier nose is circular in shape.

2. Before scour begins, the shear stress at the pier nose is approximately 4 τ_u. Here, τ_u is shear stress in the approach flow. This assumption is based on the fact that regardless of pier size, scour at pier nose begins when $u_*/u_{*c} \geq 0.5$ (Chabert and Engeldinger 1956; Hancu 1971; Hjorth 1975; Ettema 1980; Kothyari 1989).

3. As a first approximation, the following relationship is valid for the diameter of the primary vortex

$$\frac{D_v}{D} = 0.28\left(\frac{b}{D}\right)^{0.85} \quad (1)$$

Where b = the pier diameter. The experimental data of Baker (1979), Qadar (1980), Muzzamil et al. (1989) and the present study have led to the development of this relationship (see Fig. 2). Fig. 2 reveals that the size of the horseshoe vortex is also affected by the opening ratio, α. Eq. (1) may be seen to be valid for a pier in a wide channel and data with smaller opening ratios plot consistently above the line corresponding to (1). The data of Baker (1979) apply to a laminar horseshoe vortex and, hence, less weight has been given to Baker's data in obtaining (1).

4. Throughout the process of scour, the upstream half of the scour hole can be approximated as an inverted frustum of a right circular cone having an angle of frustum equal to the angle of repose of bed sediment, ϕ.

5. As the scour hole develops, the primary vortex sinks into it and expands (Melville 1975). The cross-sectional area of this vortex is assumed to be equal to the area of cross section of the scour hole plus the initial cross-sectional area of the primary vortex (Melville 1975). Thus A_t, which is the cross-sectional area of the primary vortex at any time t, is given by:

$$A_t = A_0 + A_s \quad (2a)$$

where

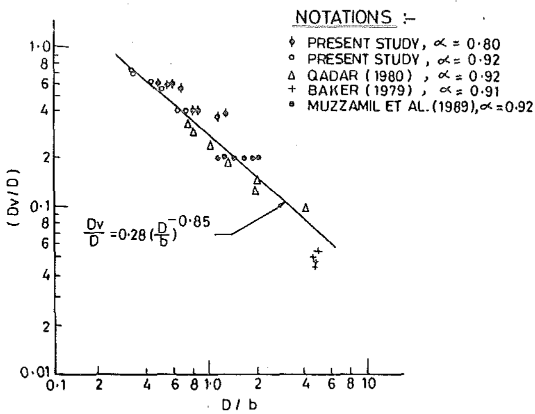

FIG. 2. Variation of (D_v/D) with (D/b)

$$A_0 = \frac{\pi}{4} D_v^2 \qquad (2b)$$

and

$$A_s = \frac{D_s^2}{2} \cot \phi \qquad (2c)$$

where A_0 = the cross-sectional area of the primary vortex at time $t = 0$; and A_s = the cross-sectional area of the scour hole when the scour depth is D_s. The value of ϕ can be assumed to be 30° for computational purposes.

6. Due to this increase in the cross-sectional area of the vortex, the shear stress under the vortex decreases (Hjorth 1975; Melville 1975). Assumption (2) stated earlier can thus be employed to describe the temporal variation of bed shear stress at the nose of the pier as scour progresses in the following manner:

$$\tau_{p,t} = 4.0\tau_u \left(\frac{A_0}{A_t}\right)^{C_1} \qquad (3)$$

where $\tau_{p,t}$ = the bed shear stress at the pier nose at time t; and C_1 = a coefficient. Note that as $A_t >> A_0$, $\tau_{p,t}$ becomes small. Obviously, the scour would cease when $\tau_{p,t}$ tends to τ_c, the critical shear stress for the material.

Estimation of Time Required for Removal of Single Sediment Particle

Following Paintal (1971), the time t_*, required by a single sediment particle to move may be expressed by:

$$t_* = \frac{C_2 d}{p_{o,t} \cdot u_{*,t}} \qquad (4a)$$

where

$$u_{*,t} = \sqrt{\frac{\tau_{p,t}}{\rho_f}} \qquad (4b)$$

where C_2 = another constant; d = the sediment size; $p_{o,t}$ = the average probability of movement of the particle at time t; and $u_{*,t}$ = the shear velocity at time t. According to Paintal (1971), the relationship for $p_{o,t}$ is given as

$$p_{o,t} = 0.45 \left(\frac{\tau_{p,t}}{\Delta\gamma_s d}\right)^{3.45}, \quad \text{for} \quad \left(\frac{\tau_{p,t}}{\Delta\gamma_s d}\right) \leq 0.25 \qquad (5a)$$

$$p_{o,t} = 1.0, \quad \text{for} \quad \left(\frac{\tau_{p,t}}{\Delta\gamma_s d}\right) > 0.25 \qquad (5b)$$

$$\Delta\gamma_s = \gamma_s - \gamma_f \qquad (5c)$$

where γ_f = specific weight of fluid.

Temporal Variation of Scour Depth in Clear-Water Flows

Scour Depth Variation with Time in Steady Flow with Uniform Sediment

On the basis of the premises set out previously, the following scheme has been evolved for the determination of scour depth at different times.

1. For the following characteristics and pier diameter, calculate $\tau_u (\tau_u = \gamma_f RS$, where R is the hyraulic radius and S is the energy slope) and A_0 using (1) and (2).
2. Use (3) with $t = 0$ and $D_s = 0$, to compute $\tau_{p,o}$.
3. Use (4) and (5) to get the value of t_*.
4. Scour depth D_s, after time t_* is equal to d.
5. The changed cross-sectional area of primary vortex is computed using (2).
6. The changed value of shear stress due to the development of the scour hole is computed using (3), and the changed value of average probability of movement is computed usng (5).
7. The new value of time t_*, which is now the time for the scour depth to increase from D_s to $D_s + d$ is computed using (4).
8. Steps 5–7 can be repeated to obtain the variation of scour depth with time.

The computations are stopped when the value of shear stress in the scour hole reduced to the value of the critical shear stress for the sediment particle in the scour hole.

The data were used for estimating the values of constants C_1 and C_2 appearing in (3) and (4), respectively. A two-dimensional grid search was used for this purpose. In this method, for a set of C_1 and C_2 values, the scour depth was computed using (1)–(5). The sum of squares of the difference between the scour depth so computed and the observed scour depth at given time periods was also computed for each set of C_1 and C_2 values. Since the maximum value of C_1 in (3) can be 1.0 and the minimum 0.0, the values of C_1 used were between 0.1 and 1.0 with an increment of 0.01. Similarly, the maximum and minimum values of C_2 were assumed to be between 10^{-2} and 10^{+2} and an increment of 0.05 was used. The values giving minimum error were $C_1 = 0.57$ and $C_2 = 0.05$ and, hence, these

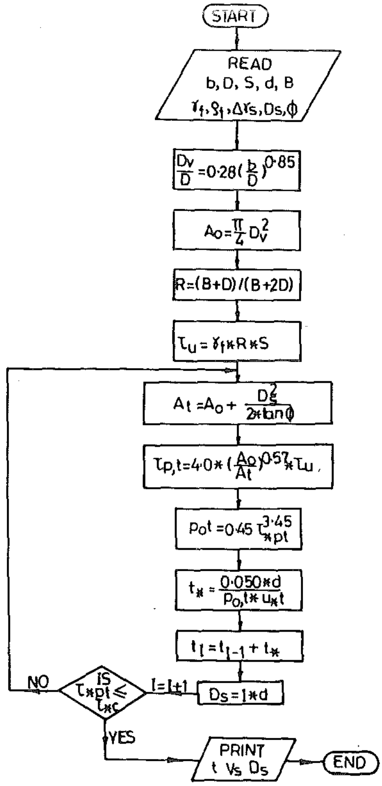

FIG. 3. Algorithm for Calculation of Temporal Variation of Scour Depth

were adopted. The flow chart for performing the computations for temporal variation of scour depth is presented in Fig. 3.

The computed scour depths using this model are compared with the observed depths for several runs (Kothyari 1989). These runs had also been included in the estimation of C_1 and C_2 as described previously. Figs. 4 and 5 show some of the results of Ettema (1980), and Chabert and Engeldinger (1956), as well as those of the writers. In some cases [Figs. 4(*a*)–4(*d*), for instance], the agreement is very good, whereas differences as large as 20% or more appear in some other cases—see Fig. 4(*e*)–4(*g*). In general, the agreement is quite satisfactory as revealed by similar plots that are shown elsewhere (Kothyari (1989)). Thus, the proposed model is considered to be well supported by the laboratory data. Islam et al. (1986) verified the relationships for temporal variation of scour depth available at the time of their study and found them to be unsatisfactory predictors over a large range of variables. One may, therefore, consider the proposed relationship to be a better predictor than the available ones.

Variation of Scour Depth with Time during Unsteady Flow with Uniform Sediments

To compute the variation of scour depth during unsteady flows, the hydrograph of flow is discretized into different segments (see Fig. 5) in which

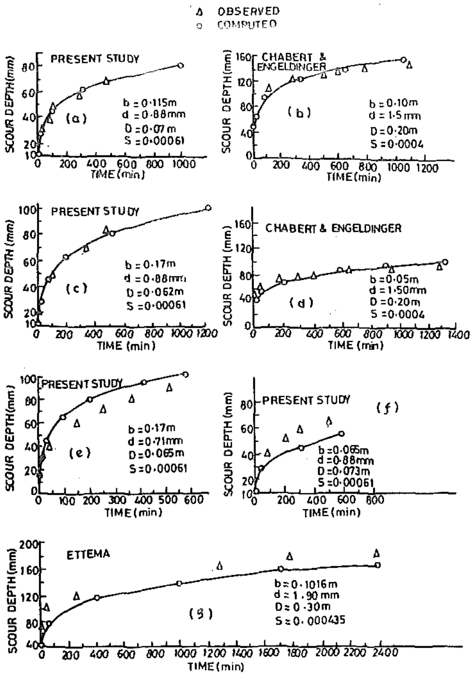

FIG. 4. Temporal Variation of Scour Depth in Uniform Sediments

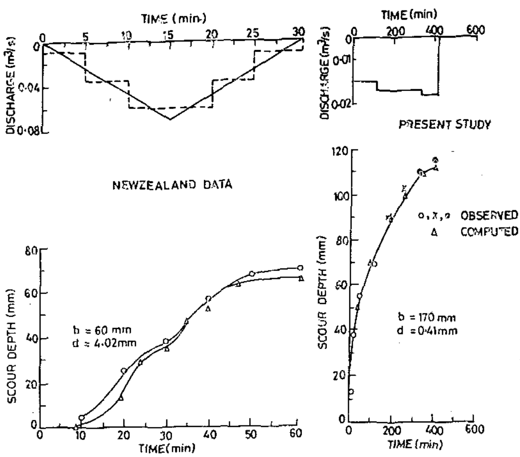

FIG. 5. Temporal Variation of Scour Depth in Unsteady Flow

the flow is assumed to be steady. The scheme for computing the variation of scour depth with time (Fig. 3) is used separately for each of these segments. The scour depth at the end of one segment becomes the scour depth at the beginning of the following segment. The data of Harwood (1977), Versatappen (1978), and Walker (1978) have been used in addition to those of the present investigation. During collection of the New Zealand data, the tail gate was completely raised during the passage of the hydrograph, thus rendering the flow nonuniform for the unsteady flow case. The energy slope for such flows would be larger than the bed slope. To use the realistic value of the energy slope in such runs, Manning's coefficient was first obtained for each set from the uniform flow data at the beginning of each run. These values of Manning's coefficient were then used to compute the energy slope for the flow in each segment of the hydrograph. In the absence of any other information, the value of velocity and the depth of flow for a given discharge in unsteady flow were taken to be the same as those for the same discharge in steady flow for which separate runs were available.

The New Zealand data indicated that a value of $\Delta t = 5$ min can be used for discretization without loss of accuracy. Typical plots showing the computed and observed variations of scour depth with time are shown in Fig. 5. A close study of these (and other plots not shown here) reveals that the proposed model gives a good estimate of the scour depth in unsteady flows. The less accurate results obtained for some of the New Zealand data may be attributed to the uncertainty in the value of energy slope as discussed previously.

Temporal Variation of Scour Depth in Nonuniform Sediments

The effective size of nonuniform sediment was defined in this study as the size of the uniform material that is scoured at the same rate as the nonuniform material under the given flow and pier conditions; thus it is the uniform size that yields agreement between the measured scour depth and that computed using the algorithm shown in Fig. 3. Using the method of grid search and the algorithm given in Fig. 3, the effective size was determined. The effective size of nonuniform material, d_{eu} is found to be equal to d_{50} for $\sigma_g \leqslant 1.124$, i.e., for material that is nearly uniform. For $\sigma_g > 1.124$, regression analysis of the data of Ettema (1980) and those collected during the present study yielded

$$\frac{d_{eu}}{d_{50}} = 0.925\sigma_g^{0.67} \quad \text{for} \quad \sigma_g > 1.124 \qquad (6a)$$

Also

$$d_{eu} = d_{50} \quad \text{for} \quad \sigma_g \leqslant 1.124 \qquad (6b)$$

where σ_g = the geometric standard deviation of the mixture. The correlation coefficient for 6(a) was 0.98.

The effective size of nonuniform material was computed using (6) for all the data. The algorithm shown in Fig. 3 was then used for computation of the temporal variation of scour depth using d_{eu} as the sediment size. A comparison between computed and observed scour depths is shown for two cases in Fig. 6. A study of these and other such plots (not shown here) reveals that use of (6) and the algorithm shown in Fig. 3 results in a reasonable estimate of the temporal variation of scour depth in nonuniform sediments. In case of the nonuniform sediment, the finer fraction of the material is scoured rapidly, and the coarser fraction is either scoured slowly or not at all. This results in progressive coarsening of the sediment in the scour hole and armoring. The process is not, of course, completely modeled by the concept of effective size as decribed previously.

J. Hydraul. Eng., 1992, 118(8): 1091-1106

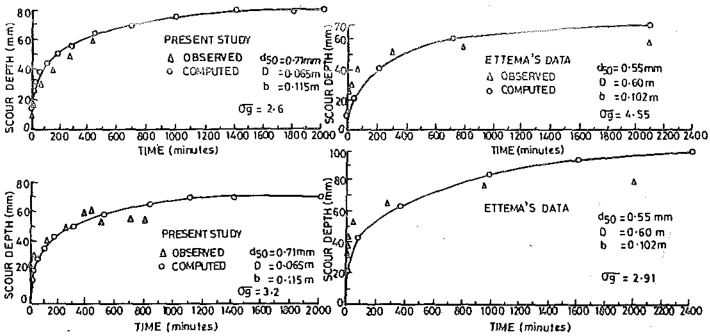

FIG. 6. Variation of Scour Depth with Time in Nonuniform Sediments

Temporal Variation of Scour Depth in Stratified Sediments

Stratification with a coarser layer at the top often exists in gravel-bed streams (Melville 1975). The temporal variation of scour in the top layer of such a bed can be obtained using the algorithm shown in Fig. 3 for uniform sediment. After the top layer is completely scoured scour begins in the bottom layer, during which the particles of the top coarser layer from upstream of the pier fall into the scour hole. The coarse sediment particles thus form an armor coat over the finer sediment of the bottom layer. Obviously, when the thickness of the top layer of coarser material is larger than the maximum scour depth for that size there will be no effect of the lower layer on the scour rate.

The effective size of the bottom finer layer of the stratified bed, d_{es}, was defined as the size of the uniform sediment that is scoured at the same rate under the given flow and pier conditions as the bottom finer layer of the stratified bed. For the data on stratified sediments of Ettema (1980) and those collected during the present investigation, d_{es} was determined using the grid search method. The effective size of the bottom finer material, d_{es}, can be defined by the following functional relationship:

$$\frac{d_{es}}{d_2} = f\left(\frac{d_1}{d_2}, \frac{h}{D_{sc1}}\right) \quad \text{(7)}$$

where d_1 = the size of top coarse material; d_2 = the size of the bottom finer material; h = the thickness of the top layer; and D_{sc1} = the maximum scour depth for top material. The graphic plotting and multiple-regression analysis gave the following equation for d_{es}:

$$\frac{d_{es}}{d_2} = 0.687\left(\frac{d_1}{d_2}\right)^{0.77}\left(1 + \frac{h}{D_{sc1}}\right)^{0.7} \quad \text{(8)}$$

The multiple correlation coefficient for (8) was 0.98. The temporal variation of scour depth for stratified sediments was computed using the scheme shown in Fig. 3 with the representative size obtained using (8) for the bottom finer material. The variation of computed and observed scour depths with time is shown for a few cases in Fig. 7. A study of these and similar other plots (not shown here) reveals that the model reasonably predicts scour in case of stratified beds with a coarser layer on top of a finer one.

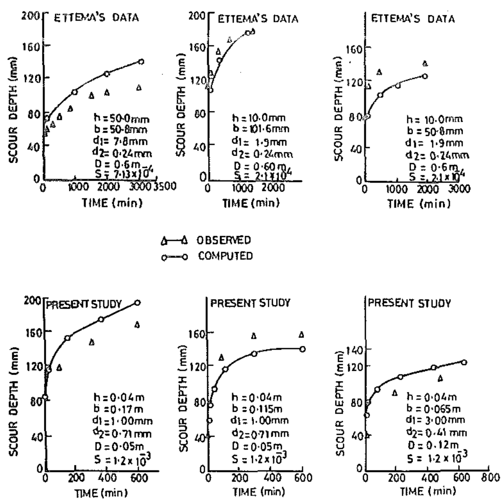

FIG. 7. Temporal Variation of Scour Depth in Stratified Sediments

Maximum Scour Depth

Uniform Sediments

The maximum scour depth can be obtained from the model as the scour depth at large t. It is, however, desirable from practical considerations to have a simple relationship for the maximum scour depth. Substituting for the various terms in the right-hand side of (3) and rearranging yields the following functional relationship for scour depth:

$$\frac{D_s^2}{b^{1.7}D^{0.3}} = f\left(\frac{\tau_0}{\Delta\gamma_s d}\right)\left(\frac{u_{*,o}\cdot t_*}{d}\right) \quad \text{(9)}$$

The shear stress in turbulent flows over rough boundaries is proportional to the square of the velocity; hence, the scour depth can be considered to be proportional to the square of approach flow velocity U. Also, the scour around bridge piers starts only when the approach flow velocity is greater than some average velocity U_c. Thus, the excess shear stress near the pier that would be responsible for scour can be considered to be proportional to $U^2 - U_c^2$. Also, the size of the primary vortex increases as the pier spacing is reduced due to greater concentration of flow (see Fig. 2). Hence, when pier spacing is significantly reduced, the scour depends on the opening ratio, α. Thus, the functional relationship for equilibrium scour depth for clear-water scour (D_{sc}) can be written in the following form:

$$\frac{D_{sc}}{b} = f\left(\frac{b}{d}, \frac{D}{d}, \frac{U^2 - U_c^2}{\left(\frac{\Delta\gamma_s}{\rho_f}\right)d}, \alpha\right) \quad \text{(10)}$$

where $\alpha = (B - b)/B$, B = the center-to-center spacing between the piers. The data collected by Arunachalam (1965), Laursen and Toch (1956), Chitale (1962), Hancu (1971), Liu et al. (1961), Chabert and Engeldiner (1956),

J. Hydraul. Eng., 1992, 118(8): 1091-1106

Knight (1975), Jain and Fisher (1980), Ettema (1980), Walker (1978), Harwood (1977), Versatappen (1978), Chee (1982), Chiew (1984), and Shen et al. (1969) have been used to obtain the relationship for D_{sc}/b in accordance with (10). Data of some investigators, namely, Chitale (1962), Shen et al. (1969), Laursen and Toch (1956), Hancu (1971), and Arunachalam (1965) were not originally classified as clear-water scour or scour with sediment transport. Shields' criterion for incipient motion and the Manning-Strickler equation were used for classifying these into the appropriate category. Multiple regression analysis of the data gives the following equation for U_c:

$$\frac{U_c^2}{\left(\frac{\Delta\gamma_s}{\rho_f}\right) d} = 1.2 \left(\frac{b}{d}\right)^{-0.11} \left(\frac{D}{d}\right)^{0.16} \quad \text{(11)}$$

The multiple correlation coefficient for (11) is 0.85. By multiple regression analysis of data, the expression for D_{sc} is obtained as

$$\frac{D_{sc}}{b} = 0.66 \left(\frac{b}{d}\right)^{-0.25} \left(\frac{D}{d}\right)^{0.16} \left(\frac{U^2 - U_c^2}{\frac{\Delta\gamma_s}{\rho_f} d}\right)^{0.4} \alpha^{-0.3} \quad \text{(12)}$$

The coefficient of determination for (12) is 0.91. Eq. (12) is applicable only when $U > U_c$. Obviously $D_{sc} = 0$, when $U \leq U_c$. As may be seen from Fig. 8, (12) gives less than $\pm 50\%$ error for all the data. Eq. (12) becomes an enveloping equation to all the data if the constant 0.66 is replaced by 1.0. Kothyari et al. (1988) verified the relationships for maximum scour in clear-water flow given by Shen et al. (1969), Ettema (1980), Jain (1981), and Laursen and Toch (1956). The plots showing comparison of observed values of scour depths with computed ones by these equations are given by Kothyari et al. (1988). A comparison of these plots with Fig. 8 reveals that the accuracy of (12) is much better than that of the relationships

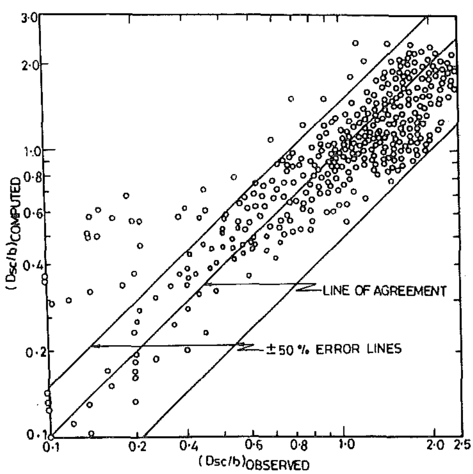

FIG. 8. Comparison of Observed Values of (D_{sc}/b) with Values Computed from (12) Clear-Water Scour with Uniform Sediment

of Shen et al. (1969), Ettema (1980), Jain (1981), and Laursen and Toch (1956). While practically all the data fall within a $\pm 50\%$ band, only 40%–60% of the data fall within such a band using the other methods.

Nonuniform Sediments

Based on the data collected by Ettema (1980), Raudkivi (1984) presented a graphic relationship between the geometric standard deviation of the sediment mixture following the lognormal distribution and a factor K_σ, which is the ratio of the maximum scour depth in nonuniform material to the maximum scour depth in uniform material having the same d_{50} as the nonuniform material. A plot of the data of the present investigation on Randkivi's (1984) graph between K_σ and σ_g (not shown here) reveals the validity of Raudkivi's relationship for σ_g values between 2 and 3. However, significant deviation occurs for σ_g less than 2 and greater then 4. Hence, modification in the plot between K_σ and σ_g is required for small values of σ_g ($\sigma_g < 2.0$) and for large values of σ_g ($\sigma_g > 4$).

An alternative approach is to use the concept of the effective size of nonuniform sediment, which has been defined earlier as the uniform size that is scoured at the same rate as the nonuniform material. Computations of the maximum scour depth using (12) with a value of effective size as given by (6) supports this notion. This procedure produces results with less than $\pm 20\%$ error for all the data (Kothyari 1989). Hence, in the absence of any other information Eqs. (6) and (12) may be used to compute the equilibrium depth in case of nonuniform sediments.

Conclusions

The primary vortex in front of the pier has been considered the prime agent causing scour. The scheme developed for the computation of temporal variation of scour depth in uniform sediments with steady flows is shown in Fig. 3. The values of constants to be used in the scheme have been determined as $C_1 = 0.57$ and $C_2 = 0.05$. This scheme predicts the temporal variation of scour depth in steady flow with satisfactory accuracy. The scheme also gives satisfactory results for scour during unsteady flows when the hydrograph causing unsteadiness is approximated by segments in which the flow is assumed to be steady.

For nonuniform sediments, the effective size has been defined as that uniform sediment size that is scoured at the same rate as the given nonuniform material under similar hydraulic conditions. The effective size of nonuniform material is related to the median size and the geometric standard deviation in (6). The proposed scheme along with (6) enables computation of the temporal variation of scour depth in nonuniform materials. The process of scour in stratified sediments having two layers with the coarser one at the top has also been studied. The effective size for the bottom, finer layer has been found to be related to the ratio of the sizes of layered sediments and the thickness of the top coarse material; see (8). The proposed scheme along with (8) give satisfactory results for the temporal variation of scour depth in stratified sediments.

Eq. (12) has been developed for the estimation of maximum scour depth in case of uniform sediment. When the effective size given by (6) is used as the sediment diameter in (12), it gives the maximum scour depth in case of nonuniform sediments.

J. Hydraul. Eng., 1992, 118(8): 1091-1106

Appendix I. References

Arunachalam, K. (1965). "Scour around bridge piers." *J. Indian Road Congress*, 251.

Baker, C. J. (1979). "Laminar horseshoe vortex." *J. Fluid Mech.*, 95(2), 317–367.

Chabert, J., and Engeldinger, P. (1956). *Etude des affonillements author des piles des ponts*. Laboratoire Natonal d'Hydraulique, Chatou, France (in French).

Chee, R. K. W. (1982). "Live-bed scour at bridge piers," ME thesis, Univ. of Auckland, Auckland, New Zealand.

Chiew, Y. M. (1984). "Local scour at bridge piers. *Report No. 355*, Univ. of Auckland, Auckland, New Zealand.

Chitale, S. V. (1962). Discussion of "Scour at bridge crossing," by E.M. Laursen. *Trans.*, ASCE, 127(1), 191–196.

Ettema, R. (1980). "Scour at bridge sites." *Report No. 117*, Univ. of Auckland, Auckland, New Zealand.

Garde, R. J., and Ranga Raju, K. G. (1985). *Mechanics of sediment transportation and alluvial stream problems*. Wiley Eastern Ltd, New Delhi, India.

Hancu, S. (1971). "Sur le, calcul des affocullements locaux dans la zone des piles du pont." *Proc. 14th Congress*, IAHR, 3, 299–313.

Harwood, N. J. (1977). "Local scour at a bridge pier caused by flood waves." ME thesis, Univ. of Canterburry, Christchurch, New Zealand.

Hjorth, P. (1975). "Studies on the nature of local scour." *Bulletin Series A, No. 46*, Lund Inst. of Tech., Lund, Sweden.

Hjorth, P. (1977). "A stochastic model for progressive scour." *Proc. of IAHR, Symp. on Stochastic Hydraulics*, Univ. of Lund, Lund, Sweden, 1977, pp. 365–383.

Islam, M. L., Gard, R. J. and Ranga Raju, K. G. (1986). "Temporal variation of local scour." *Proc. of IAHR, Symp. on Scale Effects in Modelling Sediment Transport Phenomenon*, Toronto, Canada, 253–262.

Jain, S. C. (1981). "Maximum clear-water scour around circular piers." *J. Hydr. Div.*, ASCE, 107(5), 611–626.

Jain, S. C., and Fischer, E. E. (1980). "Scour around bridge piers at high flow velocities." *J. of Hydr. Div.*, ASCE, 106(11), 1827–1842.

Knight, D. W. (1975). "A laboratory study of local scour at bridge piers." *Proc. 16th Congress,* IAHR, 2, 243–250.

Kothyari, U. C. (1989). "Scour around bridge piers," Ph.D. thesis, Univ. of Roorkee, Roorkee, India.

Kothyari, U. C., Garde, R. J. and Ranga Raju, K. G. (1988). "Maximum scour depth at circular bridge piers in clear-water flows." *6th Congress, IAHR*, Asia and Pacific Regional Division, Kyoto, Japan 261–268.

Laursen, E. M., and Toch, A. (1956). "Scour around bridge piers and abutments." *Bulletin No. 4*, Iowa Road Res. Board.

Liu, H. K., Chang, F. M. and Skinner, M. M. (1961). *Effect of bridge constriction on scour and backwater*, Engrg. Res. Ctr., Colorado State Univ., Fort Collins, Col.

Melville, B. W. (1975). "Local scour at bridge sites." *Report No. 117*, Univ. of Auckland, Auckland, New Zealand.

Muzzamil, M., Gupta, K., Gangadharaiah, T., and Subramanya, K. (1989). "Vorticity characteristics of scouring horseshoe vortex." *Proc. of 3rd Int. Workshop on Alluvial River Problems*, Roorkee, India, 19–26.

Nakagawa, H., and Suzuki, K. (1975). "An application of stochastic model of sediment motion to local scour around a bridge pier." *Proc. 16th Congress*, IAHR, Sao Paulo, Brazil, 2, 228–235.

Paintal, A. S. (1971). "A stochastic model of bed load transport." *J. Hydr. Res.*, 9(4), 91–109.

Qadar, A. (1980). "The vortex scour mechanism at bridge piers," Ph.D. thesis, Aligarh Muslim Univ., Aligarh, India.

Raudkivi, A. J. (1984). "Scour at bridge piers." *Proc. 4th Int. Conf. on Applied Numerical Modelling*, 284–289.

J. Hydraul. Eng., 1992, 118(8): 1091-1106

Shen, H. W., Ogawa, Y., and Karaki, S. K. (1965). "Time variation of bed deformation near the bridge piers. *Proc. IAHR, 11th Congress*, 3–14.
Shen, H. W., Schneider, V. R., and Karaki, S. (1969). "Local scour around bridge piers." *J. Hydr. Div.*, ASCE, 95(6) 1919–1940.
Tsujimoto, T., and Motomashi, K. (1988). "Effect of armouring on local scour around a circular cylinder." *J. of Hydrosci. Hydr. Engrg.*, 6(1), 23–33.
Verstappen, E. L. (1978). "Non steady local scour at a cylindrical pier," ME thesis, Univ. of Canterburry, Christchurch, New Zealand.
Walker, B. F. G. (1978). "Scour at a cylindrical pier by translation waves," ME thesis, Univ. of Canterburry, Christchurch, New Zealand.

Appendix II. Notations

The following symbols are used in this paper:

A_s = cross-sectional area of scour hole;
A_t = cross-sectional area of primary vortex at time t;
B = flume width or center-to-center spacing between two piers;
b = diameter of circular bridge pier;
C_1, C_2 = some constants;
D = depth of flow;
D_s = instantaneous scour depth below original bed level;
D_{sc} = maximum scour depth below original bed level;
D_{sc1} = maximum scour depth for top coarse material in stratified sediment;
D_v = diameter of primary vortex;
d = size of uniform sediment;
d_1 = uniform sediment size of top coarser layer in stratified sediments;
d_2 = uniform sediment size of bottom finer material in stratified sediments;
d_{50} = size of nonuniform material such that 50% of material is finer than this by weight;
d_{es} = effective size of bottom layer of stratified sediment;
d_{eu} = effective size of nonuniform matrial;
h = thickness of top coarser material in stratified sediment;
K_σ = ratio between maximum scour depth in nonuniform sediment to that in the uniform sediment having same size as d_{50} of nonuniform material;
$P_{o,t}$ = average probability of movement at time t;
R = hydraulic radius;
S = energy slope of approach flow;
t = time after beginning of scour when scour depth is D_s;
t_* = time required for single sediment particle to get scoured;
U = velocity of approach flow;
U_c = velocity of approach flow corresponding to inception of sediment particle motion in approach flow;
u_{*t} = shear velocity at time t;
α = opening ratio $[(B - b)/B]$;
γ_f = specific weight of fluid;
γ_s = specific weight of sediment;
Δ_t = time period chosen for discretization of hydrograph into segments representing steady flow;

J. Hydraul. Eng., 1992, 118(8): 1091-1106

ρ_f = mass density of water;
ρ_s = mass density of sediment;
σ = arithmetic standard deviation of nonuniform sediments;
σ_g = geometric standard deviation of nonuniform sediments;
$\tau_{p,t}$ = shear stress at pier nose at time t;
τ_u = shear stress in approach flow; and
ϕ = angle of respose for sediment particles.

J. Hydraul. Eng., 1992, 118(8): 1091-1106